Ultrasonics Sonochemistry 73 (2021) 105519

Contents lists available at ScienceDirect

Ultrasonics Sonochemistry

journal homepage: www.elsevier.com/locate/ultson

Synthesis of graphene oxide and graphene quantum dots from miscanthus via ultrasound-assisted mechano-chemical cracking method

Yuxin Yan [a,b], Sivakumar Manickam [c], Edward Lester [d], Tao Wu [b,e], Cheng Heng Pang [a,f,*]

[a] Department of Chemical and Environmental Engineering, University of Nottingham Ningbo China, Ningbo 315100, PR China
[b] New Materials Institute, University of Nottingham Ningbo China, Ningbo 315042, PR China
[c] Petroleum and Chemical Engineering, Faculty of Engineering, Universiti Teknologi Brunei, Bandar Seri Begawan BE1410, Brunei Darussalam
[d] Department of Chemical and Environmental Engineering, University of Nottingham, Nottingham NG7 2RD, UK
[e] Key Laboratory for Carbonaceous Wastes Processing and Process Intensification Research of Zhejiang Province, University of Nottingham Ningbo China, Ningbo 315100, PR China
[f] Municipal Key Laboratory of Clean Energy Conversion Technologies, University of Nottingham Ningbo China, Ningbo 315100, PR China

ARTICLE INFO

Keywords:
Graphene oxide
Graphene quantum dots
Ultrasound
Sonication
NMP
Exfoliation

ABSTRACT

Whilst graphene materials have become increasingly popular in recent years, the followed synthesis strategies face sustainability, environmental and quality challenges. This study proposes an effective, sustainable and scalable ultrasound-assisted mechano-chemical cracking method to produce graphene oxide (GO). A typical energy crop, miscanthus, was used as a carbon precursor and pyrolysed at 1200 °C before subjecting to edge-carboxylation via ball-milling in a CO_2-induced environment. The resultant functionalised biochar was ultrasonically exfoliated in *N*-Methyl-2-pyrrolidone (NMP) and water to form GOs. The intermediate and end-products were characterised via X-ray diffraction (XRD), Raman, high-resolution transmission electron microscopy (HR-TEM) and atomic force microscopy (AFM) analyses. Results show that the proposed synthesis route can produce good quality and uniform GOs (8–10% monolayer), with up to 96% of GOs having three layers or lesser when NMP is used. Ultrasonication proved to be effective in propagating the self-repulsion of negatively-charged functional groups. Moreover, small amounts of graphene quantum dots were observed, illustrating the potential of producing various graphene materials via a single-step method. Whilst this study has only investigated utilising miscanthus, the current findings are promising and could expand the potential of producing good quality graphene materials from renewable sources via green synthesis routes.

1. Introduction

The emergence of graphene, an allotrope of carbon in a 2D structure, promises a faster, better and more efficient future. This single layer of sp^2-hybridized carbon atoms (and its derivatives) brings with it a string of unrivalled characteristics at a fraction of the price of its competitors, which includes platinum. Apart from having extraordinary electrical, thermal and mechanical properties, graphene is also known to be tougher than diamond and stronger than steel. Yet, it is flexible like rubber and remains as the thinnest material on Earth. Unsurprisingly, graphene and its derivatives have been extensively studied across a wide range of disciplines and industries, and their potential is becoming more apparent.

Particularly, graphene oxide (GO) and graphene quantum dots (GQDs) are two highly explored graphene materials. GO has a heterogeneous structure in which the contiguous aromatic lattice of graphene is interrupted by oxygen-containing functional groups [1]. These functional groups improve hydrophilicity, aqueous dispersibility, and structural diversity [2–4], thus widening the application of graphene materials in the field of composite, energy storage and biomedicine [5,6]. GQDs are regarded as zero-dimensional graphene derivatives with dimensions below 100 nm in diameter [7]. Like graphene, GQDs have excellent physicochemical properties with enhanced biocompatibility and strong quantum characteristic, thereby allowing them to excel in nanomedicine and bio-imaging applications. Whilst the graphene market is expected to grow at an astonishing compound annual growth rate (CAGR) of approximately 40% in the next seven years [8], there seems to be a challenge in meeting the demands from such growth. The industrialisation and commercialisation of graphene production are still limited by product quality, yield, costs, process safety and scalability,

* Corresponding author at: Department of Chemical and Environmental Engineering, University of Nottingham Ningbo China, Ningbo 315100, PR China.
E-mail address: chengheng.pang@nottingham.edu.cn (C.H. Pang).

https://doi.org/10.1016/j.ultsonch.2021.105519
Received 16 December 2020; Received in revised form 28 February 2021; Accepted 5 March 2021
Available online 13 March 2021

and environmental considerations.

One of the most popular methods is top-down exfoliation, which could be achieved either mechanically or chemically, or both. In order to separate graphite into different layers of graphene, an average energy input of more than 2 eV/nm graphene surface is needed to overcome the van der Waals forces [9]. The noble-prize-winning scotch tape method falls under the category of 'micromechanical exfoliation'. The use of adhesive tape to peel off carbon nanomaterials is simple and effective; however, this manual method is inefficient and has no control over the size and thickness of the graphene [10]. On the other hand, mechanical shear exfoliation is a more scalable alternative with a higher production yield. Exfoliation is known to occur in both regimes of laminar and turbulent flow when the local shear rate exceeds 10^4 s^{-1} [11,12]. On a small laboratory scale, such shear rates could be easily achieved using a domestic kitchen blender. However, graphene produced via shearing is usually thick and multilayered, i.e. low aspect ratio with a lateral size of 300–800 nm and an average of seven layers [12].

Chemical exfoliation is known for its reliability and suitability for upscaling [13]. The chemical method involves oxidising graphite by introducing oxygen into the layered structure in the form of carboxyl, carbonyl, hydroxyl and/or epoxide functional groups [9,14]. These oxygen-containing functional groups increase the interlayer spaces within graphite and facilitate the delamination of nanocrystalline graphene oxide [15]. The Hummers' method is a well-studied example [16]. However, the initial oxidation stage introduces structural defects leading to damage and disruption of the conjugation of the carbon basal plane [7,11]. Moreover, chemical exfoliation is highly dependent on harsh and hazardous chemicals and has been reported to yield lower quality graphene materials [5].

To circumvent quality and hazardous issues, few researchers have explored direct exfoliation in an appropriate liquid [17–20]. An appropriate liquid refers to a solvent with surface energy similar to that of graphene, i.e. 68 mJ/m^2 [21,22]. Such direct liquid exfoliation is reported to produce defect-free graphene [21]. Until recently, more than 50 different types of solvents have been studied for the exfoliation of graphene [23–25]. However, *N*-Methyl-2-pyrrolidone (NMP) remains one of the best solvents to disperse graphene [9]. For better exfoliation, ultrasonication is commonly used to promote the separation of graphene layers [9,21,26,27]. Instantaneous conditions of up to 5000 K, 20 MPa and rapid heating-cooling rates of 10^9 $K.s^{-1}$ have been reported during sonication [28]. Such harsh yet desirable conditions create shock waves that could dismantle graphite into graphene layers [9]. However, sonication-assisted exfoliation is reported to have a low yield with a production rate as low as 0.04 $g.h^{-1}$ [12], which poses a challenge for large-scale production.

The most common starting material for top-down methods is graphite, which occurs naturally in igneous and metamorphic rocks. However, natural graphite production is faced with (1) depletion of ore reserves [29], (2) declining and limited mining activities, particularly in countries outside China, India, Brazil and Mexico, (3) stricter enforcement of environmental regulations and policies, and (4) increasing community rejection to mining. These have led to an increase in the costs of graphite mining and, hence, graphite. On the contrary, biomass is a renewable, sustainable, and widely available alternative to graphite as a potential carbon precursor to graphene materials. However, careful processing is required to convert biomass into a carbon material which is ready for exfoliation.

Whilst there are other investigations on producing GOs from biomass, the resultant GOs are commonly in the range of 6–8 layers [30,31] and usually involve some form of harsh chemical processing. This study investigates the potential of synthesising good quality and yield of graphene materials from miscanthus via an effective, sustainable, and scalable method without utilising any harsh and toxic chemicals. Specifically, this study aims to (1) propose a novel ultrasound-assisted mechano-chemical cracking method for the synthesis of high quality and yield of graphene materials; (2) establish the potential of converting miscanthus into highly graphitic, oriented bio-char as a carbon precursor to graphene oxide; (3) investigate the effects of polar solvents (water and NMP) on the yield and quality of resultant graphene materials, thereby enabling a balance between efficiency and health, safety and environment (HSE).

2. Materials and method

2.1. Synthesis of biochar

Milled miscanthus particles (<200 μm) were graphitised via high-temperature pyrolysis in a laboratory tubular furnace (GSL-1700x). The biomass sample was heated under constant nitrogen (99.99% N_2) gas flow of 120 ml/min at 5 °C/min to a final temperature of 1200 °C. The total heating time was 240 min whilst the final holding time at final temperature was 60 min.

2.2. Characterisation of biochar

The chemical structure of biochar was characterised via Raman spectroscopy. Raman measurements were performed from 200 to 4000 cm^{-1} at room temperature using a Raman spectrometer (Renishaw Series RM2000) equipped with a 514 nm laser excitation source. The degree of graphitisation and crystallinity were examined via X-ray diffraction (XRD) patterns obtained from monochromatic CuKα radiation (Bruker D8 A25) at 40 kV and 35 mA between 10° and 90° (2θ) at a scanning rate of 0.02°/s (2θ).

2.3. Mechano-chemical cracking of biochar

Mechano-chemical cracking of biochar was carried out in a planetary ball mill (Droide, PM4L) fitted with a 1.5 kW motor delivering a nominal rotational speed of 500 rpm. 1 g of biochar, 100 g of dry ice and 300 g of aluminium oxide balls (5 mm diameter) were placed into a stainless steel capsule. The container was then sealed and fixed in the planetary ball mill and agitated for 48 h. The internal pressure was maintained at 5 bar by a pressure control valve. The resultant product was washed with 1 M aqueous HCl solution to remove metallic impurities and further freeze-dried (FD-1A-50) at −50 °C under the pressure of <6 Pa for 48 h.

2.4. Synthesis of graphene oxide

The resultant bio-precursor was added into NMP (≥99.0%, Sigma-Aldrich) solution (20 wt%) or DI water. The mixture was sonicated (KS-9983, 40 kHz) for 1 h in an ice bath and centrifuged at 1500 rpm for 45 min. The supernatant was collected for high-resolution transmission electron microscopy (HR-TEM) and atomic force microscopy (AFM) analyses. Then, the supernatant was filtered through a 0.22 μm polytetrafluoroethylene (PTFE) membrane with a vacuum pump (SHB-III) and freeze-dried (FD-1A-50) at −50 °C under the pressure of <6 Pa for 48 h.

2.5. Characterisation of graphene oxide

The morphology and structure of the as-prepared GO nanosheets were characterised by HR-TEM, AFM and Raman spectra. HR-TEM (JEM-2100) was used to cross-examine the morphological and textural features of GO at an accelerating voltage of 200 kV. A drop of GO suspension was placed onto a carbon-coated copper grid (300 mesh) and then dried under ambient conditions before TEM analysis at a resolution of 5 nm. TEM images were further processed using the ImageJ software (v 1.51r) to determine the interlayer spacing. AFM (Daojing, SPM-9700) was used to quantify the morphological properties of individual GO flakes, including the number of layers and thickness. A drop of GO suspension was deposited onto a silicon substrate and dried under ambient conditions before analysis. In this study, AFM was carried out,

in parallel with HR-TEM, to determine the number of graphene layers based on the measurements from a minimum of 100 flakes per sample. Similarly, the chemical structure of GO was examined via Raman spectroscopy as described in Section 2.2.

3. Results and discussion

3.1. Synthesis of biochar

In this study, biomass was used as the starting material and carbon precursor to synthesise graphene oxide. Miscanthus, a typical perennial energy crop, was first pyrolysed to concentrate the carbon elements in the solid products, i.e. biochar. Whilst the pyrolysis of biomass for energy conversion has been widely studied [32–35], pyrolysis of biomass for graphene synthesis is limited. Amongst the multiple factors influencing pyrolysis, temperature is the most significant in determining the properties of biochar [36,37]. Preliminary study has shown that 1200 °C is the optimum pyrolysis temperature (for miscanthus) to produce highly oriented, pyrolytic biochar resembling graphite. The ability to transform biomass into graphitic biochar is crucial and desirable for subsequent exfoliation. Moreover, previous studies have reported that the surface area and pore volume of biochar are largest at 1200 °C, and with no significant reduction in char yield compared to lower pyrolysis temperatures [38]. Thus, the property of biochar is important in influencing the feasibility of graphene production and, if feasible, the property of the resultant graphene.

3.1.1. Characterisation of biochar

XRD was used to study the degree of carbon ordering and crystallinity of biochar samples. The XRD pattern for biochar pyrolysed at 1200 °C (BC-1200) is shown in Fig. 1. The broad peak at 23.5° is due to the crystal plane index C(0 0 2), which, in turn, is related to the parallel and azimuthal orientation of the aromatic and carbonised structure. The sharp peak indicates a high degree of orientation. Moreover, the high symmetry of the C(0 0 2) peak indicates the absence of γ-bands linked to amorphous and aliphatic structures [39]. Another broad peak is observed at 43.5°, assigned to C(1 0 0) diffractions of graphitic and hexagonal carbons, which reflect the size of the aromatic lamina [40]. The sharp C(1 0 0) peak is an indication of a high degree of aromatic ring condensation. The XRD results show that biochar obtained at 1200 °C is highly graphitic and aromatic, which is desirable for effective exfoliation.

Raman spectroscopy was used to further characterise the structural features of biochar. Fig. 2 illustrates the Raman spectrum of the biochar

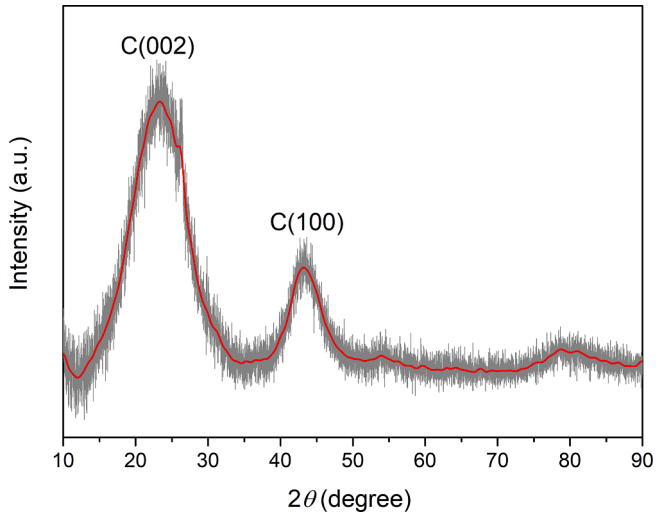

Fig. 1. XRD pattern of the obtained biochar.

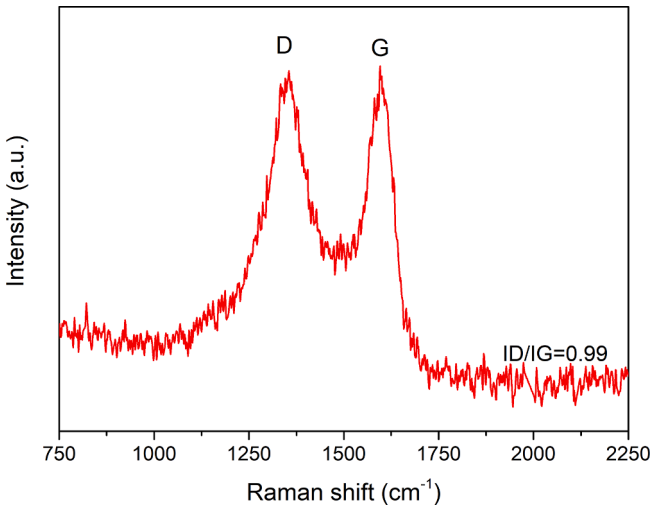

Fig. 2. Raman spectrum of the obtained biochar.

obtained at 1200 °C, showing two bands at 1354 cm^{-1} (D band) and 1596 cm^{-1} (G band). The D band is associated with disordered carbon structures, whilst the G band is related to the vibration of sp^2-hybridized carbon atoms in graphitic carbon layers [41]. The distinct and sharp peaks indicate a high degree of carbon ordering.

Pyrolysis temperature plays a crucial role in determining the carbon structuring of biochar, and hence its suitability for subsequent exfoliation. Too low a temperature leads to incomplete graphitisation thus preserving the amorphous, aliphatic and complex biomass cellular structure, whilst too high a temperature results in a significant loss of 'defects' as the aromatic ring system continuously increases to more than six fused benzene rings due to the continuous ring condensation. Moreover, high temperatures also result in the loss of functional groups, such as carbonyl and hydroxyl groups [42], thus further reducing the number of defects. This would lead to a net reduction in the I_D/I_G ratio, and a more compact biochar structure which requires more energy during exfoliation. The I_D/I_G ratio of 0.99 suggests that the biochar obtained at 1200 °C has an adequate degree of carbon ordering yet contains the sufficient number of functional groups to increase the interspacing between pyrolytic layers for effective exfoliation. Moreover, 1200 °C is an optimum temperature for balancing between biochar quality, quantity, and energy consumption.

3.2. Synthesis of graphene oxide

The highly pyrolytic, oriented biochar was first edge-functionalised via the mechano-chemical cracking method, followed by ultrasonic-assisted exfoliation in polar solvents, leading to the formation of few-layer graphene oxide. Effective functionalisation is crucial in ensuring effective exfoliation. Biochar was subjected to ball-milling in a controlled CO_2 environment which is the precursor to carboxylate functional groups. The fast mechanical movements within the milling chamber provide the necessary energy and conditions to initiate chemical reactions. The high impact and shearing of the grinding media, coupled with abundant CO_2 in the surrounding, create instantaneous temperature and pressure leading to the mechano-chemical cracking of graphitic carbon-carbon bonds in the biochar. This is followed by spontaneous chemical incorporation of carboxylate groups at the broken edges of the carbon network of biochar, resulting in edge-functionalisation.

By utilising the mechano-chemical cracking method, no harsh chemicals are needed [43]. More importantly, better control of functionalisation and defects could be achieved as foreign entities are only introduced at the edges compared to the entire basal plane, as seen in chemical functionalisation methods [44]. The continuous impact and

shearing also mean that no heating element is required. This is contrary to the more traditional methods which require high temperature (above 800 °C) and processing costs [45,46].

It has been reported that functionalisation is decidedly more challenging compared to exfoliation [47], and the exfoliation process has a deterministic effect on the quality and quantity of the resultant graphene materials. The similar charges of the carboxylate groups create mutual repulsion in polar solvents, thus initiating exfoliation at the biochar edges. Moreover, ultrasound irradiation was applied to provide the necessary energy and conditions to further propagate the exfoliation extending from the edges. Tests without ultrasound irradiation did not record obvious yield of GOs within the same processing time. Sonication could facilitate and accelerate the exfoliation of functionalised biochar into graphene oxide layers owing to the associated acoustic cavitation effect. Ultrasonic waves create a large number of tiny bubbles that expand in the low pressure region whilst contracting rapidly in the high pressure region. These microcavities form, grow and collapse violently, thus creating instantaneous temperature as high as 5000 K [48] and pressure over 100 MPa [49]. Such intense and discontinuous condition creates shock waves that could propagate exfoliation initiated at the repelled edges. Moreover, microturbulence and pitting effects during the collapse of bubbles result in high-speed liquid jets and shear forces with mechanical energy in excess to the van der Waals forces between pyrolytic layers, thereby contributing to the successful exfoliation [50].

In this study, two different polar solvents (NMP and deionised water) were used to investigate the effects on the exfoliation process. NMP is known to be one of the most effective polar solvents for graphene exfoliation [25] and would be a good candidate to investigate if the proposed ultrasonic-assisted mechano-chemical cracking method works, particularly on biochar. On the other hand, water is a cleaner, safer and cheaper alternative to the expensive and carcinogenic NMP. Hence this study provides an insight into the tradeoff between feasibility, health and safety.

3.2.1. Characterisation of graphene oxide

The HR-TEM was used to perform semi-quantitative analysis on the morphology and microstructure of the resultant GOs. Fig. 3 illustrates the high magnification HR-TEM micrographs of GO sheets exfoliated from biochar. GO-NMP-1200 and GO-H_2O-1200 represent GOs obtained from sonication in NMP and DI water, respectively. Both samples show a highly ordered and oriented carbon structure, which is typical of graphene materials. Most GO sheets display a semi-transparent appearance with wrinkles and foldings around the edges, indicating high flexibility and low thickness, particularly below ten layers [51]. This suggests that the proposed method is effective in deriving GO from biomass.

As shown in the HR-TEM micrographs, the interlayer spacing of each sample was determined via image analysis on the GO sheet edges. On average, GO-H_2O-1200 and GO-NMP-1200 have an interlayer spacing of 0.391 nm and 0.399 nm, respectively, which is within the expected normal range [52,53]. Typically, the interlayer spacing of GOs is larger

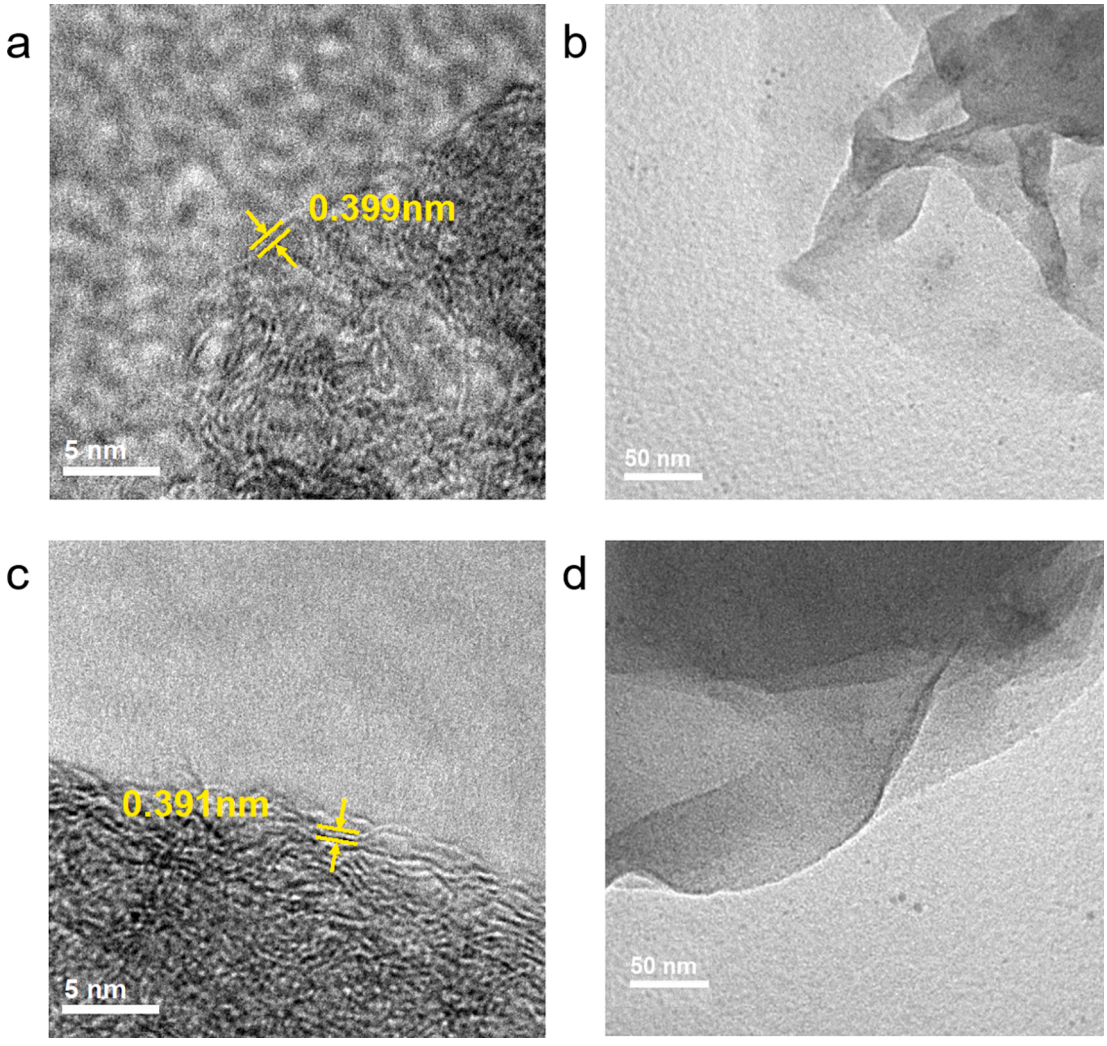

Fig. 3. HR-TEM micrographs of GO sheets obtained from sonication in NMP (a and b) and in DI water (c and d). (a) and (c) illustrate the interlayer spacing, respectively.

than that of pure graphite (0.335 nm) [54] due to the functional groups extending the distance between pyrolytic layers. This has been observed in GOs in previous reports [55,56]. The ionisation of carboxylate groups incorporated during ball milling and the carbon-, hydrogen- and oxygen-containing functional groups inherited from biomass and bio-char tend to be negatively charged and lead to mutual repulsions thus increasing the interlayer distance. This was also observed in previous works [57]. Also, ultrasonication results in high-velocity liquid jets and vibration derived waves which are known to weaken van der Waals forces [30] and can further increase the interlayer spacing between the carbon layers.

It would appear, based on the number of wrinkle fringes, that GO-NMP-1200 has a fewer number of layers compared to GO-H_2O-1200. This is partly due to the larger interlayer distance in GO-NMP-1200 that has resulted in weaker interlayer interaction forces, and hence increases the ease of exfoliation. NMP is known to have similar surface energy to graphene materials and can penetrate and intercalate into the pyrolytic layers as wedges to separate the layers [58]. The similarity in surface energy also reduces the tendency of GO sheets to 'restack' into overlapped aggregates, contrary to the water-sonicated samples, due to the strong van der Waals force associated with the defect-free basal planes and hydrogen bonding of the edge-carboxylic acids [57]. Moreover, previous studies have reported a strong, positive correlation between interlayer spacing and solubility [59]. This suggests that the interlayer spacing in GO-NMP-1200 is naturally larger than that in GO-H_2O-1200 due to the higher solubility of GOs in NMP. Hence, NMP is a more effective polar solvent in the ultrasonic-assisted exfoliation to form few-layer GO sheets.

The atomic force microscopy (AFM) is a direct and visual analytical method to examine the topographical and cross-sectional features of graphene materials. In this study, AFM was carried out, in parallel to HR-TEM, to determine the number of GO layers. Fig. 4 shows the AFM images of GO sheets exfoliated in different polar solvents. In general, the GO sheets possess an elongated sheet structure inherited from biomass fibres. However, the thickness of each sample significantly varies, ranging from 0.449 nm to 4.091 nm, indicating GO sheets of single to few layers. Specifically, taking into account the interlayer spacing from HR-TEM analysis (Fig. 4), the average number of GO layer was calculated (based on the thickness of 100 sheets per sample) and shown as a statistical histogram in Fig. 5. It appears that both GO-H_2O-1200 and GO-NMP-1200 have a mode of two layers (the value with the highest frequency).

Moreover, both samples have a similar proportion of monolayer GO at 10% and 8%, respectively, which is similar to a typical GO synthesis from graphite. This indicates the potential of deriving good quality few-layer GOs from pyrolysed biomass. However, GO-H_2O-1200 has a wider thickness distribution ranging from monolayer to more than ten layers, whilst GO-NMP-1200 has a narrower range of 1–4 layers. On average, GO-NMP-1200 has a lesser overall thickness, with 96% of the GO sheets having three or fewer layers, compared to GO-H_2O-1200 with only 48%.

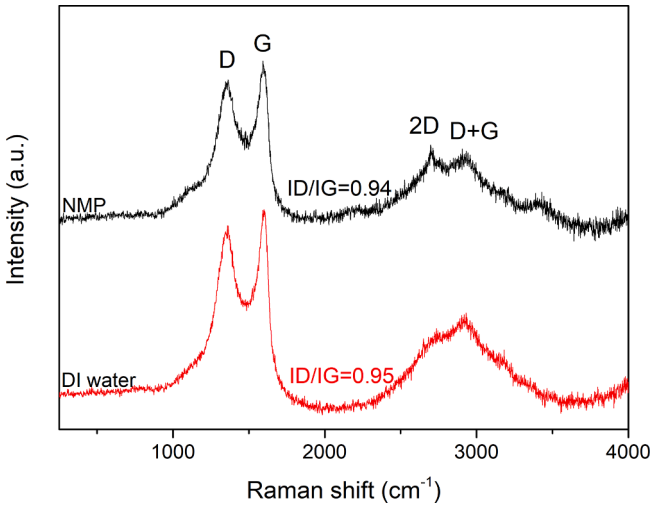

Fig. 5. Raman spectra and corresponding I_D/I_G ratios of GO sheets.

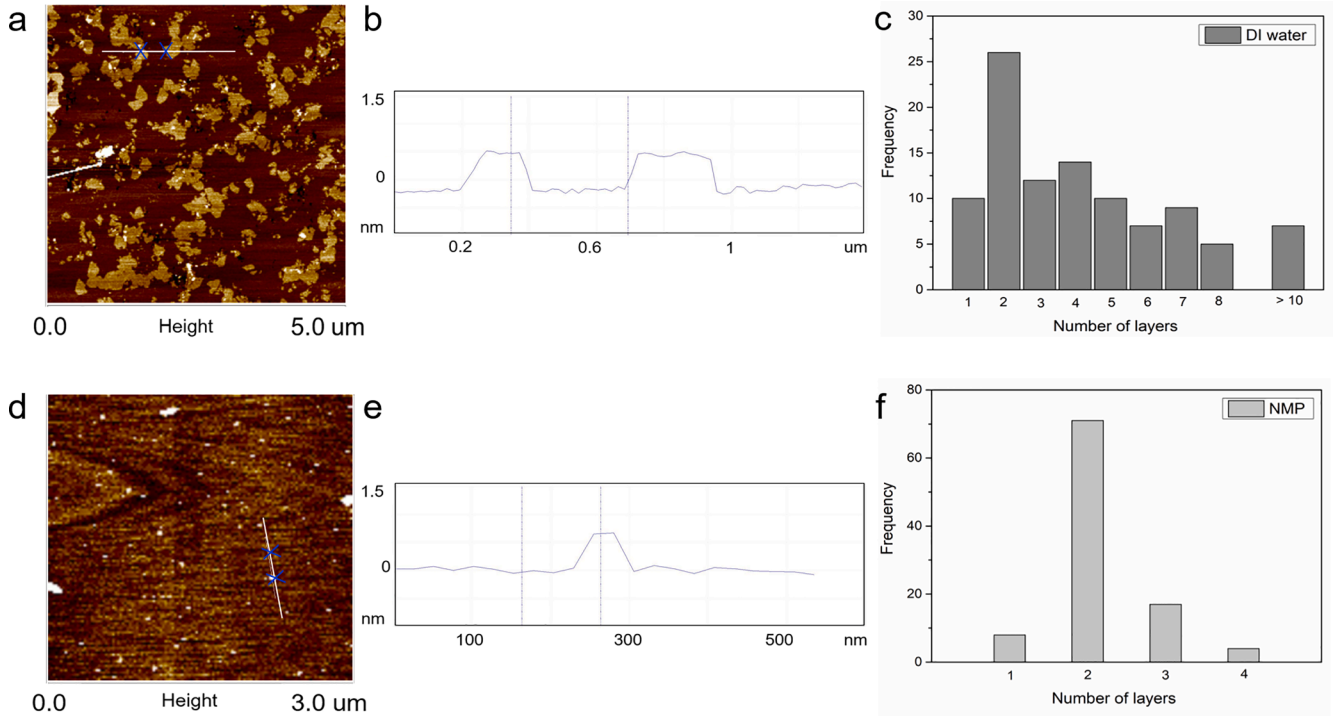

Fig. 4. AFM analysis: Top row for GO sheets obtained from sonication in NMP whilst bottom row for GO sheets obtained from sonication in DI water. (a and d) AFM images; (b and e) height profile across the white line in AFM images; (c and f) histogram illustrating the statistical thickness distribution of GO sheets.

NMP provides stronger interactions between the solvent and GO sheets, promoting exfoliation and subsequent solvation by decreasing the required energy [25]. This suggests that NMP is a more effective polar solvent for exfoliation, compared to water, to yield uniform, consistent and thin GO sheets.

Similar to biochar, the non-destructive Raman spectroscopy was used to examine the chemical and crystal structures of the resultant GOs. Fig. 5 shows the Raman spectra and corresponding I_D/I_G ratios of GOs. Two prominent peaks are visible, corresponding to the D band at around 1360 cm^{-1} which is activated by the disruption of symmetry at defects and edges. The G band at 1598 cm^{-1} is due to in-plane C–C deformation [60]. The discernible bands located at approximately 2697 cm^{-1} and 2905 cm^{-1} are identified as 2D and D + G bands, which are typical for GO materials [61,62]. The 2D band is associated with the overtone of the D band, whilst the D + G band corresponds to the combination mode induced by disorder effects [63]. The 2D band of graphene-based materials is valuable for distinguishing monolayer graphene from bilayer/multilayer graphene as it is highly perceptive to stacking. Monolayer graphene has a Lorentzian peak at 2679 cm^{-1}, whilst the peak of multilayer graphene is broad and located at a higher wavenumber [64]. In our study, the 2D peaks of GO-H_2O-1200 and GO-NMP-1200 are observed at 2737 cm^{-1} and 2697 cm^{-1}, respectively. The higher wavenumber and a broader 2D peak of GO-H_2O-1200 suggest multi-layered structure due to stacking or re-stacking of GO layers in water. On the other hand, the sharp and narrow 2D peak of GO-NMP-1200 is indicative of mono- or bilayer structure. NMP is known to provide better thermodynamic stabilisation, compared to water, for the dispersion of graphene material due to its surface energy matching with that of graphitic materials [65]. This is particularly true for GOs due to the presence of polar edge-carboxylic groups that would increase dispersibility in higher polarity solvent like NMP [57].

In general, the I_D/I_G ratios of the exfoliated samples (0.94–0.95) are relatively smaller than that of biochar (0.99). This is due to the loss of edge-functionalisation during sonication, thereby reducing defects and improving the average size of sp^2 domains. However, the I_D/I_G ratio of GO-NMP-1200 is marginally smaller than that of GO-H_2O-1200. Exfoliation occurs more readily in NMP than in water leading to more complete GO sheets with a lower degree of defects.

3.2.2. *Potential of producing graphene quantum dots*

Whilst this study has established the potential of producing good quality and uniform GOs from biomass using the proposed method, an interesting finding shows that there might be further potential with this study. Small amounts of graphene quantum dots were also produced and observed in the exfoliated samples. The GQDs are embedded within the wrapped GO sheets with dimensions of about 6 nm, as demonstrated in Fig. 6. The measured inter-planar spacings of GQDs-NMP-1200 and GO-H_2O-1200 are 0.223 and 0.241 nm, respectively, which agree well with the literature values [7,66]. Whilst the exact mechanism of carbon dot formation has yet to be established or disclosed [67], it is possible that the observed GQDs were formed as a result of 'overprocessing' during the GO synthesis. Both ball milling and ultrasonication, via continuous shearing, impact, and cavitation, could induce cracking of large sp^2 carbon domains of the edge-functionalised biochar and GOs into smaller units capable of exhibiting quantum confinement effects. Moreover, the abundant oxygen-containing functional groups attached at the edges and defect sites of the carbon basal plane are known to be 'fragile' and serve as active sites allowing GOs to be cleaved into GQDs [68,69]. Whilst the yield of such GQDs is not significantly large, it does demonstrate potential in deriving graphene materials from renewable sources, and appropriate operating conditions may improve yield and selectivity during synthesis.

4. Conclusions

This study aims to promote and integrate the concept of sustainability in the synthesis of graphene materials by (1) using renewable carbon sources in replacement of the more commonly used fossil graphite, and (2) using a more sustainable polar solvent. Hence, the effectiveness of water as a polar solvent during exfoliation was studied against the more effective, yet carcinogenic, NMP. The findings of this study clearly demonstrate that the proposed ultrasound-assisted mechano-chemical cracking method provides a viable route to synthesise good quality and consistent GOs (8–10% monolayer), particularly when NMP is used. It is acknowledged that whilst water is clean and safe, the expensive NMP is twice as effective as a polar solvent to yield up to 96% GOs with three layers or lesser. NMP can effectively penetrate and intercalate between pyrolytic biochar layers leading to more complete GO sheets with a lower degree of defect (lower I_D/I_G ratio). Ultrasonication is effective in promoting and propagating the mutual repulsion of functional groups of like-charges, leading to a better exfoliation rate compared to non-sonicated procedures. This study has also established the potential of biomass, a sustainable and readily available alternative to graphite, as a carbon precursor to graphene materials. Hence, the proposed synthesis method is a green, effective and scalable route to produce high-quality graphene oxide and graphene quantum dots. However, careful consideration should be given when choosing a polar solvent. Moreover, this study still leaves an unanswered question of how to control the yield and quality of graphene materials, and the significance of processing conditions, particularly temperature and

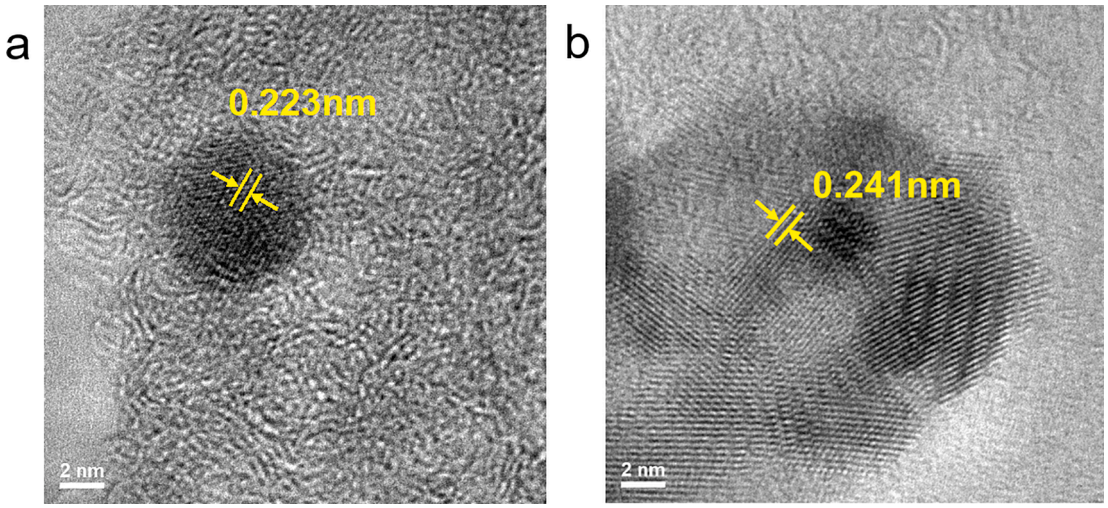

Fig. 6. HR-TEM micrographs of GQDs obtained from sonication in (a) NMP and (b) DI water.

residence time. Still, this study does form the basis of future studies, both in terms of experiments and theories, to further explore the full potential of renewable sources in producing advanced materials.

CRediT authorship contribution statement

Yuxin Yan: Conceptualization, Data curation, Formal analysis, Investigation, Methodology, Visualization, Writing - original draft. **Sivakumar Manickam:** Methodology, Visualization, Validation, Writing - review & editing. **Edward Lester:** Validation, Writing - review & editing. **Tao Wu:** Supervision, Validation, Resources, Writing - review & editing. **Cheng Heng Pang:** Conceptualization, Formal analysis, Investigation, Methodology, Writing - original draft, Resources, Supervision, Writing - review & editing.

Declaration of Competing Interest

The authors declare that they have no known competing financial interests or personal relationships that could have appeared to influence the work reported in this paper.

Acknowledgements

The authors gratefully express gratitude to all parties who have contributed towards the success of this project, both financially and technically, especially the S&T Innovation 2025 Major Special Programme (grant number 2018B10022) and the Ningbo Natural Science Foundation Programme (grant number 2018A610069) funded by the Ningbo Science and Technology Bureau, China, as well as the UNNC FoSE Faculty Inspiration Grant, China. The Zhejiang Provincial Department of Science and Technology is also acknowledged for this research under its Provincial Key Laboratory Programme (2020E10018).

References

[1] P. Gholami, et al., A review on carbon-based materials for heterogeneous sonocatalysis: fundamentals, properties and applications, Ultrason. Sonochem. 58 (2019), 104681.
[2] F. Kim, L.J. Cote, J. Huang, Graphene oxide: surface activity and two-dimensional assembly, Adv. Mater. 22 (17) (2010) 1954–1958.
[3] D.C. Marcano, et al., Improved synthesis of graphene oxide, ACS Nano 4 (8) (2010) 4806–4814.
[4] J. Jia, et al., Green synthesis of biocompatiable chitosan–graphene oxide hybrid nanosheet by ultrasonication method, Ultrason. Sonochem. 32 (2016) 300–306.
[5] R. Geetha Bai, et al., Acoustic cavitation induced generation of stabilizer-free, extremely stable reduced graphene oxide nanodispersion for efficient delivery of paclitaxel in cancer cells, Ultrason. Sonochem. 36 (2017) 129–138.
[6] B. Neppolian, et al., Graphene oxide based Pt–TiO_2 photocatalyst: ultrasound assisted synthesis, characterization and catalytic efficiency, Ultrason. Sonochem. 19 (1) (2012) 9–15.
[7] P. Russo, et al., Femtosecond laser ablation of highly oriented pyrolytic graphite: a green route for large-scale production of porous graphene and graphene quantum dots, Nanoscale 6 (4) (2014) 2381–2389.
[8] Graphene Market Size, Share & Trends Analysis Report By Application (Electronics, Composites, Energy), By Product (Graphene Nanoplatelets, Graphene Oxide), By Region, And Segment Forecasts, 2020–2027.
[9] Y. Wei, Z. Sun, Liquid-phase exfoliation of graphite for mass production of pristine few-layer graphene, Curr. Opin. Colloid Interface Sci. 20 (5–6) (2015) 311–321.
[10] K. Mylvaganam, L. Zhang, Graphene nanosheets: mechanisms for large-area thin films production, Scr. Mater. 115 (2016) 145–149.
[11] E. Varrla, et al., Turbulence-assisted shear exfoliation of graphene using household detergent and a kitchen blender, Nanoscale 6 (20) (2014) 11810–11819.
[12] K.R. Paton, et al., Scalable production of large quantities of defect-free few-layer graphene by shear exfoliation in liquids, Nat. Mater. 13 (6) (2014) 624–630.
[13] H.N. Tien, et al., Enhanced solvothermal reduction of graphene oxide in a mixed solution of sulfuric acid and organic solvent, Chem. Eng. J. 211–212 (2012) 97–103.
[14] Q. Yan, Q. Liu, J. Wang, A simple and fast microwave assisted approach for the reduction of graphene oxide, Ceram. Int. 42 (2 Part B) (2016) 3007–3013.
[15] T.V. Khai, et al., Direct production of highly conductive graphene with a low oxygen content by a microwave-assisted solvothermal method, Chem. Eng. J. 232 (2013) 346–355.
[16] W.S. Hummers, R.E. Offeman, Preparation of graphitic oxide, J. Am. Chem. Soc. 80 (6) (1958), 1339–1339.
[17] Y. Hernandez, et al., High-yield production of graphene by liquid-phase exfoliation of graphite, Nat. Nano 3 (9) (2008) 563–568.
[18] A. Ciesielski, P. Samorì, Graphene via sonication assisted liquid-phase exfoliation, Chem. Soc. Rev. 43 (1) (2014) 381–398.
[19] W. Du, X. Jiang, L. Zhu, From graphite to graphene: direct liquid-phase exfoliation of graphite to produce single- and few-layered pristine graphene, J. Mater. Chem. A 1 (36) (2013) 10592–10606.
[20] X. Cui, et al., Liquid-phase exfoliation, functionalization and applications of graphene, Nanoscale 3 (5) (2011) 2118–2126.
[21] Y. Arao, et al., G12 Mass production of high-aspect-ratio few-layer-graphene by high-speed laminar flow, Carbon 102 (2016) 330–338.
[22] J.N. Coleman, Liquid exfoliation of defect-free graphene, Acc. Chem. Res. 46 (1) (2013) 14–22.
[23] L. Fernández-García, et al., Morphological changes in graphene materials caused by solvents, Colloids Surf., A 558 (2018) 73–79.
[24] J. Ma, et al., Solubility study on the surfactants functionalized reduced graphene oxide, Colloids Surf. A: Physicochem. Eng. Aspects 538 (2018) 79–85.
[25] Y. Hernandez, et al., High-yield production of graphene by liquid-phase exfoliation of graphite, Nat. Nanotechnol. 3 (9) (2008) 563–568.
[26] A. Hadi, et al., Optimization of graphene production by exfoliation of graphite in supercritical ethanol: a response surface methodology approach, J. Supercrit. Fluids 107 (2016) 92–105.
[27] C.E. Halbig, et al., Quantitative investigation of the fragmentation process and defect density evolution of oxo-functionalized graphene due to ultrasonication and milling, Carbon 96 (2016) 897–903.
[28] K.S. Suslick, L.A. Crum, Sonochemistry and sonoluminescence, in: Encyclopedia of Acoustics, John Wiley & Sons Inc, 2007, pp. 271–281.
[29] A.D. Jara, et al., Purification, application and current market trend of natural graphite: a review, Int. J. Mining Sci. Technol. 29 (5) (2019) 671–689.
[30] S.S. Shams, et al., Synthesis of graphene from biomass: a green chemistry approach, Mater. Lett. 161 (2015) 476–479.
[31] T. Purkait, et al., Large area few-layer graphene with scalable preparation from waste biomass for high-performance supercapacitor, Sci. Rep. 7 (1) (2017) 15239.
[32] Y. Yan, et al., Ignition and kinetic studies: the influence of lignin on biomass combustion, Energy Fuels 33 (7) (2019) 6463–6472.
[33] Y. Yan, et al., The kinetics studies and thermal characterisation of biomass, Energy Proc. 158 (2019) 357–363.
[34] C.H. Pang, et al., Relationship between thermal behaviour of lignocellulosic components and properties of biomass, Bioresour. Technol. 172 (2014) 312–320.
[35] C.H. Pang, E. Lester, T. Wu, Influence of lignocellulose and plant cell walls on biomass char morphology and combustion reactivity, Biomass Bioenergy 119 (2018) 480–491.
[36] J. Zhang, J. Liu, R. Liu, Effects of pyrolysis temperature and heating time on biochar obtained from the pyrolysis of straw and lignosulfonate, Bioresour. Technol. 176 (2015) 288–291.
[37] Y. Li, et al., A critical review of the production and advanced utilization of biochar via selective pyrolysis of lignocellulosic biomass, Bioresour. Technol. 312 (2020) 123614.
[38] K. Zeng, et al., The effect of temperature and heating rate on char properties obtained from solar pyrolysis of beech wood, Bioresour. Technol. 182 (2015) 114–119.
[39] L. Lu, et al., Char structural ordering during pyrolysis and combustion and its influence on char reactivity, Fuel 81 (9) (2002) 1215–1225.
[40] I. Mansuri, et al., Carbon dissolution using waste biomass—a sustainable approach for iron-carbon alloy production, Metals 8 (2018) 290.
[41] K. Krishnamoorthy, G.-S. Kim, S.J. Kim, Graphene nanosheets: ultrasound assisted synthesis and characterization, Ultrason. Sonochem. 20 (2) (2013) 644–649.
[42] Y. Yin, et al., Effect of char structure evolution during pyrolysis on combustion characteristics and kinetics of waste biomass, J. Energy Res. Technol. 140 (2018) 072203.
[43] O. Mondal, et al., Reduced graphene oxide synthesis by high energy ball milling, Mater. Chem. Phys. 161 (2015) 123–129.
[44] D.W. Boukhvalov, M.I. Katsnelson, Chemical functionalization of graphene with defects, Nano Lett. 8 (12) (2008) 4373–4379.
[45] Y. Zhi, et al., Sulfur-doped graphene as an efficient metal-free cathode catalyst for oxygen reduction, ACS Nano 6 (1) (2011) 205–211.
[46] S. Yang, et al., Efficient synthesis of heteroatom (N or S)-doped graphene based on ultrathin graphene oxide-porous silica sheets for oxygen reduction reactions, Adv. Funct. Mater. 22 (22) (2012) 3634–3640.
[47] P. Yu, et al., Electrochemical exfoliation of graphite and production of functional graphene, Curr. Opin. Colloid Interface Sci. 20 (5-6) (2015) 329–338.
[48] A. Abulizi, K. Okitsu, J.-J. Zhu, Ultrasound assisted reduction of graphene oxide to graphene in l-ascorbic acid aqueous solutions: kinetics and effects of various factors on the rate of graphene formation, Ultrason. Sonochem. 21 (3) (2014) 1174–1181.
[49] X. Gu, et al., Method of ultrasound-assisted liquid-phase exfoliation to prepare graphene, Ultrason. Sonochem. 58 (2019), 104630.
[50] K. Muthoosamy, S. Manickam, State of the art and recent advances in the ultrasound-assisted synthesis, exfoliation and functionalization of graphene derivatives, Ultrason. Sonochem. 39 (2017) 478–493.
[51] L.R. Melo de Lima, et al., Characterization of commercial graphene-based materials for application in thermoplastic nanocomposites, Mater. Today: Proc. 20 (2020) 383–390.
[52] Y. Song, et al., Ultrapermeable graphene oxide membranes with tunable interlayer distances via vein-like supramolecular dendrimers, J. Mater. Chem. A 7 (31) (2019) 18642–18652.

[53] S. Park, et al., Hydrazine-reduction of graphite- and graphene oxide, Carbon 49 (9) (2011) 3019–3023.
[54] T. Soltani, B.-K. Lee, Low intensity-ultrasonic irradiation for highly efficient, eco-friendly and fast synthesis of graphene oxide, Ultrason. Sonochem. 38 (2017) 693–703.
[55] D.G. Trikkaliotis, A.C. Mitropoulos, G.Z. Kyzas, Low-cost route for top-down synthesis of over- and low-oxidized graphene oxide, Colloids Surf., A 600 (2020), 124928.
[56] V.H. Pham, et al., Chemical functionalization of graphene sheets by solvothermal reduction of a graphene oxide suspension in N-methyl-2-pyrrolidone, J. Mater. Chem. 21 (10) (2011) 3371–3377.
[57] I.-Y. Jeon, et al., Edge-carboxylated graphene nanosheets via ball milling, Proc. Natl. Acad. Sci. U.S.A. 109 (15) (2012) 5588–5593.
[58] L. Liu, et al., Synergistic effect of supercritical CO_2 and organic solvent on exfoliation of graphene: experiment and atomistic simulation studies, Phys. Chem. Chem. Phys. 21 (39) (2019) 22149–22157.
[59] S. Zheng, et al., Correlating interlayer spacing and separation capability of graphene oxide membranes in organic solvents, ACS Nano 14 (5) (2020) 6013–6023.
[60] A.C. Ferrari, D.M. Basko, Raman spectroscopy as a versatile tool for studying the properties of graphene, Nat. Nanotechnol. 8 (4) (2013) 235–246.
[61] D. Konios, et al., Dispersion behaviour of graphene oxide and reduced graphene oxide, J. Colloid Interface Sci. 430 (2014) 108–112.
[62] C.T.J. Low, et al., Electrochemical approaches to the production of graphene flakes and their potential applications, Carbon 54 (2013) 1–21.
[63] E. Dervishi, et al., Raman spectroscopy of bottom-up synthesized graphene quantum dots: size and structure dependence, Nanoscale 11 (35) (2019) 16571–16581.
[64] S. Thakur, N. Karak, Green reduction of graphene oxide by aqueous phytoextracts, Carbon 50 (14) (2012) 5331–5339.
[65] X. Cui, et al., Liquid-phase exfoliation, functionalization and applications of graphene, Nanoscale 3 (5) (2011) 2118–2126.
[66] A. Abbas, et al., High yield synthesis of graphene quantum dots from biomass waste as a highly selective probe for Fe3+ sensing, Sci. Rep. 10 (1) (2020).
[67] R. Kumar, V.B. Kumar, A. Gedanken, Sonochemical synthesis of carbon dots, mechanism, effect of parameters, and catalytic, energy, biomedical and tissue engineering applications, Ultrason. Sonochem. 64 (2020), 105009.
[68] L.-L. Li, et al., A facile microwave avenue to electrochemiluminescent two-color graphene quantum dots, Adv. Funct. Mater. 22 (14) (2012) 2971–2979.
[69] G. Rajender, P.K. Giri, Formation mechanism of graphene quantum dots and their edge state conversion probed by photoluminescence and Raman spectroscopy, J. Mater. Chem. C 4 (46) (2016) 10852–10865.